Wobbling excitations in odd-A nuclei with high-j aligned particles

Ikuko Hamamoto
Department of Mathematical Physics, Lund Institute of Technology at the University of Lund, Lund, Sweden
(Received 27 November 2001; published 12 March 2002)

Using the particle-rotor model in which one high-j quasiparticle is coupled to the core of triaxial shape, wobbling excitations are studied. The family of wobbling phonon excitations can be characterized by: (a) very similar intrinsic structure while collective rotation shows the wobbling feature; (b) strong $B(E2;I\rightarrow I-1)$ values for $\Delta n_w=1$ transitions where n_w expresses the number of wobbling phonons. For the Fermi level lying below the high-j shell with the most favorable triaxiality $\gamma\approx+20°$, the wobbling phonon excitations may be more easily identified close to the yrast line, compared with the Fermi level lying around the middle of the shell with $\gamma\approx-30°$. The spectroscopic study of the yrast states for the triaxial shape with $-60°<\gamma<0$ are illustrated by taking a representative example with $\gamma=-30°$, in which a quantum number related with the special symmetry is introduced to help the physics understanding.

DOI: 10.1103/PhysRevC.65.044305 PACS number(s): 21.10.Re, 23.20.−g

I. INTRODUCTION

The nuclear wobbling mode, which is uniquely related to triaxiality of nuclear shape [1], has been experimentally searched for years without success. Very recently [2], a firm evidence for the wobbling excitation has been obtained in the high-spin states of the nucleus $^{163}_{71}Lu_{92}$. In the wobbling motion described in the text book, for example, in Ref. [1], the only angular momentum in the system is the total angular momentum. In contrast, the possible presence of the angular momentum coming from the intrinsic motion can in many ways make the nuclear wobbling mode much richer in its structure. A microscopic description of the nuclear wobbling motion was attempted first in Ref. [3]. The presence of high-j aligned particles favors a particular (triaxial) shape [4] and produces a unique pattern of electromagnetic transitions between bands [5]. The states with high-j aligned particles can lie in the neighborhood of the yrast line, because of the relatively small rotational energy needed for constructing a given angular momentum due to the aligned particles.

In Ref. [2] the electromagnetic properties of several connecting transitions between two presumably triaxial, strongly deformed (TSD) bands in $^{163}_{71}Lu_{92}$ have been studied in detail. The intrinsic structure of those TSD bands is understood as containing aligned high-j ($i_{13/2}$) protons. The assignment of the excited TSD2 band as a wobbling mode built on the yrast TSD1 band is established based on, among others, the observed large $B(E2)$ values of the transitions from the $I+1$ state in TSD2 to the I state in TSD1, which are in good agreement with the result of the particle-rotor calculations. In Ref. [6] the observation of two other TSD bands, TSD3 and TSD4, is reported and the possibility of TSD3 being the two-phonon wobbling excitations is suggested. The suggestion is based, at the moment, on the agreement of observed $B(E2)$ values of the $I\rightarrow I-2$ transitions from TSD3 to TSD1 with the values calculated in the particle-rotor model, in addition to the observed moments of inertia and alignments of very similar magnitudes in those TSD bands. A further confirmation of large $B(E2)$ values of the transitions from the $I+1$ state in TSD3 to the I state in TSD2 is absolutely needed for establishing TSD3 as the two-phonon wobbling mode. The analysis of experimental data to extract the $B(E2)$ values is at present under way [7].

In Ref. [5] it is pointed out that the wobblinglike mode of the collective angular momentum of the core, which is built on the yrast favored-signature (α_f) band, may appear as the yrast unfavored-signature (α_u) band in odd-A nuclei when the high-j shell is half-filled with the triaxial shape of $\gamma=-30°$. (We use the Lund convention [8] of γ values in rotating nuclei.) The negative-parity yrast states at relatively low spins of odd-Z rare-earth nuclei, of which the configurations consist of one aligned $h_{11/2}$ proton coupled to the even-even core, satisfy the necessary condition for the appearance of the wobbling mode, if the triaxial shape with $\gamma\approx-30°$ is supported also by the core. A characteristic feature of the level scheme along the yrast line in connection with the appearance of the wobbling mode or a triaxial shape is that the yrare α_u state may appear energetically lower than the yrare α_f state [5,9]. To our knowledge, the trace of the wobbling mode was never experimentally identified in the rare-earth odd-Z nuclei. On the other hand, recent experimental data on the negative-parity states in proton-rich odd-N Xe isotopes [10] exhibit the characteristic level scheme for a triaxial shape at relatively low spins. Those negative-parity states are supposed to be consisting of one aligned $h_{11/2}$ neutron coupled to the triaxial even-even core, in which the $h_{11/2}$ shell is nearly half-filled. Thus, a question naturally arises whether the wobbling mode can be identified in those Xe isotopes. In Ref. [11] the microscopic model of nuclear wobbling motion of Ref. [3] is further developed and, then, numerical calculations are performed for several even-even nuclei including $^{124}_{54}Xe_{70}$. However, it is not clear that the numerical solution presented in Ref. [11] can be interpreted as a wobbling mode.

In Refs. [2,6] it is shown that the presently available data on the TSD2 band of ^{163}Lu can be nicely interpreted in terms of wobbling excitation with $n_w=1$ built on the yrast TSD1 band, using the particle-rotor model in which one $i_{13/2}$ quasiproton is coupled to the core of triaxial shape with $\gamma\approx+20°$. In the present work we further analyze the nature

of the states along the yrast line obtained from the particle-rotor model, taking the most favorable triaxial shape for a given degree of high-j shell filling. We are interested in the triaxial shape in three regions, $-120°<\gamma<-60°$, $-60°<\gamma<0°$, and $0°<\gamma<+60°$. In contrast to the cranking approximation, the γ values in our case are defined in connection with the axis of the largest moment of inertia. This is because in the particle-rotor model the components of collective rotation about other axes are not vanishing for a triaxial shape so that the total angular momentum is a good quantum number.

In Sec. II the model and formulas are briefly presented, while numerical results and discussions are given in Sec. III. Conclusions and further discussions are given in Sec. IV.

II. MODEL AND FORMULAS

Our intrinsic Hamiltonian is written as

$$H_{intr}=\sum_{\nu}\ (\epsilon_{\nu}-\lambda)a^{\dagger}_{\nu}a_{\nu}+\frac{\Delta}{2}\sum_{\mu,\nu}\ \delta(\bar{\mu},\nu)(a^{\dagger}_{\mu}a^{\dagger}_{\nu}+a_{\nu}a_{\mu}), \tag{1}$$

where Δ is the pair-correlation parameter in the BCS approximation and ϵ_{ν} expresses the one-particle energies for a potential V. For a single j shell we can write the triaxially deformed quadrupole potential in the form

$$V=\frac{\kappa}{j(j+1)}\{[3j_z^2-j(j+1)]\cos\ \gamma+\sqrt{3}(j_y^2-j_x^2)\sin\gamma\}, \tag{2}$$

where κ, which is proportional to the size of the quadrupole deformation β_2, is used as energy unit [12]. In order to obtain the relation between the degree of high-j shell filling and the favored intrinsic shape, we use for simplicity the cranking model. The cranking Hamiltonian is written as

$$H_{CR}=H_{intr}-\hbar\omega j_x, \tag{3}$$

taking the x axis as the cranking axis. It is shown [4] that for a given value of (λ,Δ,ω) the quasiparticle energy of H_{CR} is a minimum for $j_x=j$ and the γ value determined by

$$-2\cos(\gamma-60°)=\lambda/\kappa\ \ \text{for}\ \ -2<\lambda/\kappa<2, \tag{4}$$

where λ expresses the degree of shell filling. We note that all one-particle energy eigenvalues ϵ_{ν} of the potential (2) for a single-j shell lie well inside the region of $-2<(\epsilon_{\nu}/\kappa)<2$. (See, for example, Fig. 12.) Examples given by the relation (4) are

$$\gamma=\begin{cases}-80° & \text{for}\quad \lambda/\kappa=+1.532,\\ -30° & \text{for}\quad \lambda=0,\\ 0 & \text{for}\quad \lambda/\kappa=-1.0,\\ +20° & \text{for}\quad \lambda/\kappa=-1.532.\end{cases} \tag{5}$$

The half-filled shell, $\lambda=0$, may approximate the case of either $h_{11/2}$ protons in β-stable rare-earth nuclei or $h_{11/2}$ neutrons in proton-rich Xe isotopes. On the other hand, $\lambda/\kappa=-1.532$ for $\gamma=+20°$ expresses the Fermi level placed below the lowest one-particle energy eigenvalue in the high-j shell, while $\lambda/\kappa=+1.532$ for $\gamma=-80°$ corresponds to the Fermi level placed above the highest one-particle energy eigenvalue. The former expresses the situation of $j=i_{13/2}$ protons for the TSD bands of ^{163}Lu.

In order to understand the wobbling motion that cannot be described by the simple cranking model, we use the particle-rotor model, in which one high-j quasiparticle is coupled to the rotor. The particle-rotor Hamiltonian is written as

$$H_{PR}=H_{intr}+\sum_{k=x,y,z}\frac{\hbar^2}{2\mathfrak{J}_k}R_k, \tag{6}$$

where $\vec{R}=\vec{I}-\vec{j}$ expresses the collective rotational angular momentum of the core. Employment of the hydrodynamical moments of inertia

$$\mathfrak{J}_k=\frac{4}{3}\mathfrak{J}_0\sin^2\left(\gamma+\frac{2}{3}\pi k\right), \tag{7}$$

where the suffix k $(=1,2,3)$ on the right-hand side should be understood as k $(=x,y,z)$ on the left-hand side, automatically restricts ourselves to the rotation with $-60°<\gamma<0°$. Namely, the largest moment of inertia and, consequently, the largest component of collective rotational angular momentum is the one along the intermediate axis of the triaxial nuclear shape. In order to get a rotation with $\gamma>0$ in the particle-rotor model, we exchange [13] the moments of inertia, $\mathfrak{J}_x$ and $\mathfrak{J}_y$, obtained from the hydrodynamical model. For example, $\kappa\mathfrak{J}_0=90$ with $\gamma=+20°$ means $\kappa\mathfrak{J}_x=116$, $\kappa\mathfrak{J}_y=50$, and $\kappa\mathfrak{J}_z=14$, so that the system rotates mainly about the x axis, which is the shortest axis of the $|\gamma|=20°$ triaxial shape [1]. In order to get a rotation with $\gamma<-60°$ in the particle-rotor model, we also make a proper exchange of the components of moments of inertia so that the system rotates mainly about the longest axis of the triaxial shape.

Using the wave functions obtained from the particle-rotor model, we calculate R, R_x, and j_x defined by

$$\begin{aligned}R(R+1)&\equiv\langle R_x^2\rangle+\langle R_y^2\rangle+\langle R_z^2\rangle,\\ R_x&\equiv\sqrt{\langle R_x^2\rangle},\\ j_x&\equiv\sqrt{\langle j_x^2\rangle},\end{aligned} \tag{8}$$

where $\langle\ \rangle$ expresses the expectation values. Both I and j are good quantum numbers in the present model, while R is not.

The magnetic dipole $(M1)$ operator is written as [1]

$$\begin{aligned}M(M1,\mu)&=\sqrt{\frac{3}{4\pi}}\frac{e\hbar}{2Mc}(g_R R_{\mu}+g_l l_{\mu}+g_s s_{\mu})\\ &=\sqrt{\frac{3}{4\pi}}\frac{e\hbar}{2Mc}[g_R I_{\mu}+(g_l-g_R)l_{\mu}+(g_s-g_R)s_{\mu}].\end{aligned} \tag{9}$$

Since g_R is taken to be a constant, the contributions to $M1$ transitions come from the second and third terms in Eq. (9). We note that in the wobbling mode described in the text

book [1], in which the intrinsic angular momenta are absent, the anisotropy of the g factor is needed in order to obtain nonvanishing $M1$ transitions. The expressions of $B(M1)$ values in the presence of the anisotropy of the g factor can be found in Ref. [11], in which the theoretical formulation of rotating triaxial nuclei is taken from Ref. [14].

For $\lambda=0.0$ and $\gamma=-30°$ together with hydrodynamical moments of inertia the Hamiltonian (6) for one quasiparticle coupled to the rotor is invariant under a rotation of $\pi/2$ about the x axis [5]. That means, the wave function of each state has components with either $R_x=0,\pm4,\pm8,\ldots$ or $R_x=\pm2,\pm6,\pm10,\ldots$. Thus, we define the quantum number by

$$r_H \equiv \exp\left(\frac{i}{2}\pi R_x\right) = \begin{cases} 1 & \text{for} \quad R_x=0,\ \pm4,\ \pm8,\ldots, \\ -1 & \text{for} \quad R_x=\pm2,\ \pm6,\ \pm10,\ldots. \end{cases} \tag{10}$$

Due to the presence of the r_H quantum number, $E2$ transitions occur either by the quadrupole operator $\hat{Q}_0$ or by $\hat{Q}_2$ where the quantization axis is the x axis of the intrinsic system. Using the quadrupole moment defined in the intrinsic system [1], $Q_0 \equiv \langle \Sigma_k (2z^2-x^2-y^2)_k \rangle = (4/5)ZR^2\beta\cos\gamma$ and $Q_2 \equiv \langle \sqrt{3/2}\Sigma_k (x^2-y^2)_k \rangle = (4/5\sqrt{2})ZR^2\beta\sin\gamma$ where $0°\leqslant\gamma\leqslant60°$, we write

$$\hat{Q}_\mu = D^2_{\mu 0}Q_0 + (D^2_{\mu 2}+D^2_{\mu -2})Q_2, \tag{11}$$

which leads to $\hat{Q}_0 \propto \sin(\gamma+30°)$ and $\hat{Q}_2 \propto \cos(\gamma+30°)$ when we use the Lund convention [8] of γ values defined for $-120°\leqslant\gamma\leqslant+60°$. The $M1$ transitions between the states with different r_H quantum numbers are strictly forbidden, while the $E2$ transitions between the states with the same r_H quantum number are performed by the operator $\hat{Q}_0$ and thus vanish since $\hat{Q}_0=0$ for $\gamma=-30°$.

III. NUMERICAL RESULTS AND DISCUSSIONS

In the following we restrict the presentation of our numerical results mostly to the two sets of parameters: ($\gamma=+20°$ and $\lambda/\kappa=-1.532$) and ($\gamma=-30°$ and $\lambda=0.0$). The intrinsic shape has the largest triaxiality for $|\gamma|=30°$. The result for the parameter set, ($\gamma=-80°$ and $\lambda/\kappa=+1.532$), can be obtained from that for the set, ($\gamma=+20°$ and $\lambda/\kappa=-1.532$), using the symmetry relation between them. Moreover, the states with $-120°<\gamma<-60°$ seldom appear around the yrast line. The case of ($\gamma=-30°$ and $\lambda/\kappa=0.0$) is taken as a representative for the triaxial shape with $-60°<\gamma<0°$, since the result for the shape with large triaxiality in the region of $-40°\lesssim\gamma\lesssim-20°$ remains qualitatively the same as that for $\gamma=-30°$.

In order to obtain a simplified intuitive picture, in numerical calculations of the present work we use a pairing parameter and moments of inertia, both of which are independent of angular momentum I: $\Delta/\kappa=0.3$ and $\kappa\mathfrak{I}_0=90$. Those values are chosen so that the observed level scheme of both TSD1 and TSD2 in ^{163}Lu is, on the average, reproduced using a proper value of κ [2,6]. Though numerical results in the present work are given for $j=i_{13/2}$, it is straightforward to convert them into the case of, for example $j=h_{11/2}$, since we express the results in terms of signature quantum numbers, α_f and α_u. We designate the yrast, yrare, . . . , states with favored (unfavored) signature by α_{f1}, α_{f2}, . . . (α_{u1}, α_{u2}, . . .).

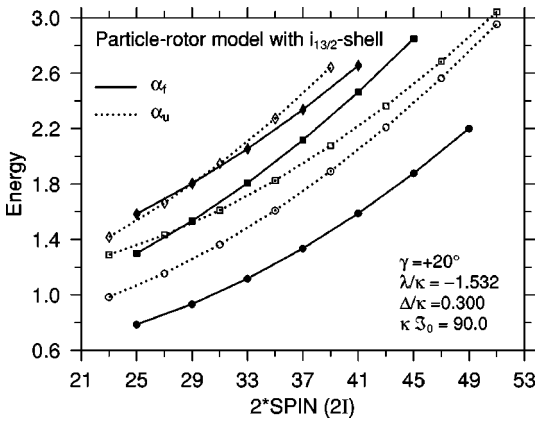

FIG. 1. Energies calculated using $\gamma=+20°$, $\lambda/\kappa=-1.532$, $\Delta/\kappa=0.3$, and $\kappa\mathfrak{I}_0=90$ are plotted as a function of I. The favored signature (α_f) bands are connected by solid lines, while the unfavored signature (α_f) bands by dotted lines.

A. The case of $\gamma=+20°$ and $\lambda/\kappa=-1.532$

In Fig. 1 the energies calculated in our particle-rotor model are shown as a function of I. The figure should be taken as a qualitative one, since the constant parameters of Δ and $\mathfrak{I}_0$ are used and since $\langle H_{intr}\rangle$ may in practice obtain an appreciable contribution by particles in shells other than the high-j shell.

In Fig. 2 we compare calculated values of R, R_x, and j_x of the α_{f1}, α_{u1}, and α_{f2} bands, respectively. It is seen that the values of R for a given I ($>23/2$) are not so different in those three bands, while the average angle between $\vec{R}$ and the x axis is nearly zero in the α_{f1} band, appreciable in the α_{u1} band, and larger in the α_{f2} band. In the α_{u3} band the angle is even larger than that of the α_{f2} band, while in Ref. [6] it is

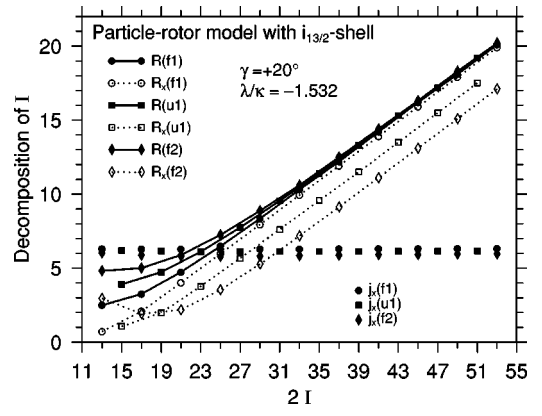

FIG. 2. Calculated values of R, R_x, and j_x, which are defined by Eq. (8), are plotted for the α_{f1}, α_{u1}, and α_{f2} bands, of which the properties show approximately those of the wobbling phonon excitations with $n_w=0$, 1, and 2.

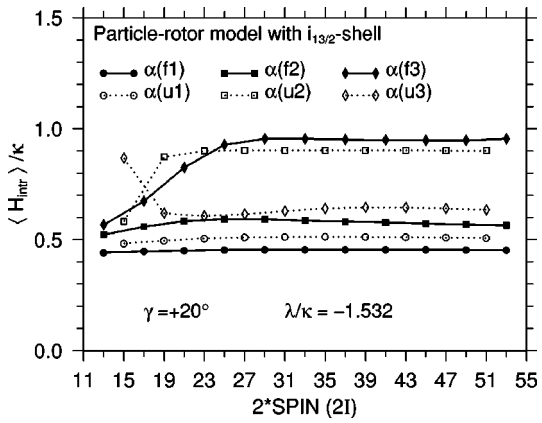

FIG. 3. Calculated expectation values of H_{intr} in Eq. (1) in the lowest three bands with α_f and those with α_u are shown for $\gamma=+20°$, $\lambda/\kappa=-1.532$, $\Delta/\kappa=0.3$, and $\kappa\mathfrak{I}_0=90$.

shown that the angle is nearly zero for the α_{u2} band. It is observed that j_x values decrease only slightly, as we go from the α_{f1} band to the α_{u1} and α_{f2} bands. In Fig. 3 the expectation value of H_{intr} as a function of I is shown for the α_{f1}, α_{f2}, α_{f3}, α_{u1}, α_{u2}, and α_{u3} bands. It is seen that the α_{f1}, α_{u1}, α_{f2}, and α_{u3} bands have clearly the lower expectation values of H_{intr} for high spins, $I>19/2$.

As explained in Refs. [5,2,6], the coupling scheme of the quasiparticle and core angular-momenta in the α_{f1} and α_{u1} bands is understood by the schematic illustration in Fig. 4, where the collective rotation about the x axis is energetically cheapest. In the lowest favored-signature band (α_{f1}) with the fully aligned particle the rotation of the core about the axis of the largest moment of inertia is energetically cheapest. If the triaxial shape is strongly favored in energy by the fully aligned high-j particle, the α_u state, which consists of the fully aligned particle and a wobbling motion of the collective rotational angular momentum of the core, may become very low in energy. When the gain in the intrinsic

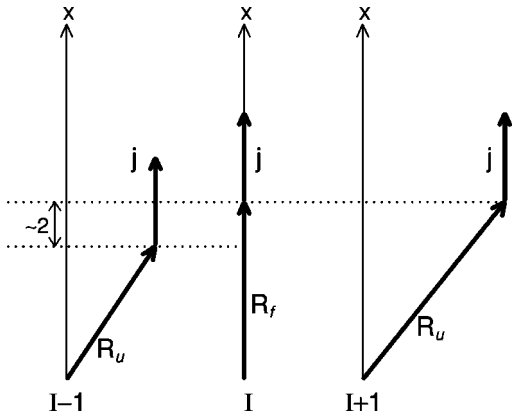

FIG. 4. Schematic illustration of the coupling scheme of the angular momenta of the high-j particle $\vec{j}$ and the core $\vec{R}$ in the yrast favored (I) state and the yrast unfavored ($I\pm1$) states of the wobbling excitation ($n_w=1$). The x axis is the axis of the largest moment of inertia of the core, about which collective rotation is energetically cheapest. The total angular momentum is $\vec{I}=\vec{R}+\vec{j}$.

energy of the high-j particle wins against the loss in the collective rotation energy of the core, the wobbling mode, which is sketched in Fig. 4, becomes the lowest α_u state (α_{u1}). We note that in the simple cranking picture the angular momentum of collective rotation $\vec{R}$ is parallel to the x axis (similar to the situation in the α_{u2} band [6]), while the particle angular momentum $\vec{j}$ in the α_u bands is always tilted. It should also be remarked that for an axially symmetric shape the collective rotation can occur only about the axis perpendicular to the symmetry axis. Then, the wobbling motion of $\vec{R}$ illustrated for the α_u bands in Fig. 4 is not possible.

The α_u states in Fig. 4 illustrate the one-phonon ($n_w=1$) wobbling mode built upon the yrast α_f state. If the triaxial shape is energetically strongly favored by the fully aligned high-j particle, one may expect that the two-phonon ($n_w=2$) wobbling excitation may appear as a low-lying α_f band, in which $\vec{j}$ is almost fully aligned while $\vec{R}$ is tilted from the x axis more than in the α_u ($n_w=1$) band. Examining Fig. 2 we may interpret the α_{f2} band as the $n_w=2$ wobbling excitation. Furthermore, evaluating the average angle between $\vec{R}$ and the x axis indicates that the α_{u3} band may be regarded as a candidate for the three-phonon ($n_w=3$) wobbling mode. The nature of many-phonon wobbling excitations should further appear in the electromagnetic decay properties, which in the absence of anharmonicity can be estimated by using those of one-phonon wobbling excitation.

In Refs. [2,6] we compare the $\Delta I=1$, $E2/M1$ transitions in the wobbling regime, from the (α_u, $n_w=1$) band to the yrast (α_f, $n_w=0$) band, with those in the case of the α_u band being in the cranking regime. It is found that the signature dependence (or the zigzag pattern) of both $B(E2)$ and $B(M1)$ values in the wobbling regime is out of phase compared with that in the cranking regime. In the wobbling regime the $\Delta I=1$ transition is dominated by $E2$ and not by $M1$. Namely, the $B(E2;I\rightarrow I-1)$ values are the order of $1/I$ in the limit of high I values [1], since the wobbling amplitude is the order of $1/\sqrt{I}$. The $B(E2;\alpha_f,n_w=0,I\rightarrow\alpha_u,n_w=1,I-1)$ values are reduced because the contributions from Q_0 and Q_2 for $\gamma=+20°$ almost cancel with each other, while $B(M1;\alpha_f,n_w=0,I\rightarrow\alpha_u,n_w=1,I-1)$ values are reduced, because of $\Delta R_x\approx2\hbar$ as seen in Fig. 4.

In Fig. 5 we show the calculated $B(E2;n_w,I\rightarrow n_w-1,I-1)/B(E2;n_w,I\rightarrow n_w,I-2)$ values between all pairs, which are the candidates for $\Delta n_w=1$ pairs in the present calculation. Though these $B(E2)$ values have a zigzag pattern as a function of I (as shown in Fig. 9), we have here plotted and connected only the larger $B(E2)$ values. For $\gamma=+20°$ those plotted in Fig. 5 are always for the $E2$ transitions with larger transition energies between the signature partners and thus can be more easily measured. In Ref. [2] it is shown that the values of $B(E2;\alpha_{u1},I\rightarrow\alpha_{f1},I-1)/B(E2;\alpha_{u1},I\rightarrow\alpha_{u1},I-2)$ in Fig. 5 plotted by filled circles with solid lines are in good agreement with the measured $B(E2;\mathrm{TSD2},I\rightarrow\mathrm{TSD1},I-1)/B(E2;\mathrm{TSD2},I,\rightarrow\mathrm{TSD2},I-2)$ values in ^{163}Lu. In the absence of anharmonicity one expects the relation $B(E2;n_w,I\rightarrow n_w-1,I-1)\approx n_wB(E2;n_w=1,I\rightarrow n_w=0,I-1)$ due to the boson nature of the wobbling phonon. Taking the ratio of the values ex-

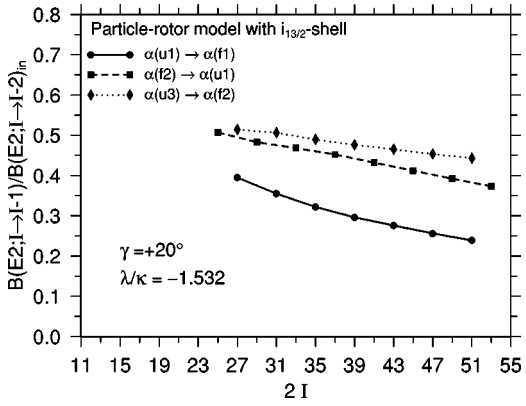

FIG. 5. Calculated $B(E2;n_w,I\rightarrow n_w-1,I-1)/B(E2;n_w,I\rightarrow n_w,I-2)$ values between the bands, $(n_w=0,\alpha_{f1})$, $(n_w=1,\alpha_{u1})$, $(n_w=2,\alpha_{f2})$, and $(n_w=3,\alpha_{u3})$, are shown for $\gamma=+20°$, $\lambda/\kappa=-1.532$. Though the $B(E2;n_w,I\rightarrow n_w-1,I-1)$ values have a signature dependence (zigzag pattern) as a function of I, only the larger $B(E2)$ values are plotted.

pressed by the solid, dashed, and dotted curves in Fig. 5, we find that anharmonicity in $B(E2)$ values is considerable. Nevertheless, the nature of many-phonon wobbling excitations with $n_w=1$, 2, and 3 in the α_{u1}, α_{f2}, and α_{u3} bands, respectively, can be traced by the unusually large $B(E2;I\rightarrow I-1)$ values at those high spins.

It is also very interesting to note that the intrinsic and rotational structure of the α_{f3} band at $I>25/2$ can be understood as the one-phonon $(n_w=1)$ wobbling excitation built on the α_{u2} band, which belongs to the cranking regime [6]. First of all, the $B(E2;\alpha_{f3},I\rightarrow\alpha_{u2},I-1)$ values are found to be large and of the same order of magnitude of the $B(E2;\alpha_{u1},I\rightarrow\alpha_{f1},I-1)$ values. Second, the average angle between $\vec{R}$ and the x axis in the α_{f3} band at $I>25/2$ indicates the characteristic feature of one-phonon wobbling excitation. Third, the expectation values of the intrinsic Hamiltonian in the α_{u2} and α_{f3} bands are indeed very similar, as shown in Fig. 3.

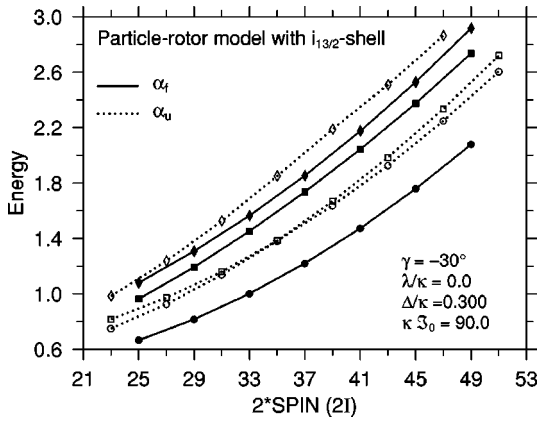

FIG. 6. Energies calculated using $\gamma=-30°$, $\lambda/\kappa=0.0$, $\Delta/\kappa=0.3$, and $\kappa\mathfrak{I}_0=90$ are plotted as a function of I. The favored signature (α_f) bands are connected by solid lines, while the unfavored signature (α_f) bands by dotted lines.

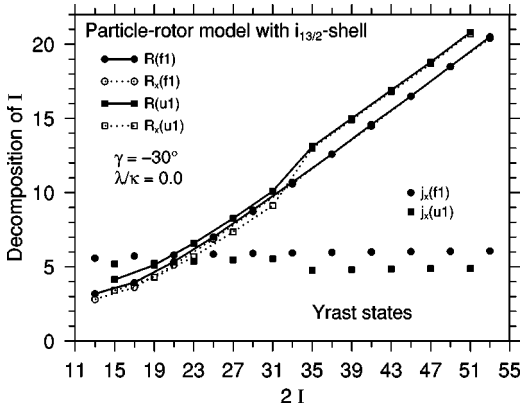

FIG. 7. Calculated values of R, R_x, and j_x, which are defined by Eq. (8), are plotted for the α_{f1} and α_{u1} bands.

B. The case of $\gamma=-30°$ and $\lambda/\kappa=0.0$

In Fig. 6 the calculated energies are shown as a function of I. The α_{u1} and α_{u2} bands cross with each other between $I=31/2$ and $I=35/2$. The interaction between the α_{u1} and α_{u2} bands is vanishing, since the states with the same I in the two bands have different r_H quantum numbers.

In Fig. 7 we compare calculated values of R, R_x, and j_x in the α_{f1} and α_{u1} bands, while in Fig. 8 those in the α_{f2} and α_{u2} bands. Examining both the relative magnitudes of R and R_x and the absolute magnitude of j_x, it is clearly seen that the α_{u1} band for $I\leqslant 31/2$ and the α_{u2} band for $I\geqslant 35/2$ have the nature of one-phonon wobbling excitation built on the yrast α_{f1} band. In contrast, in the α_{u1} band for $I\geqslant 35/2$ and the α_{u2} band for $I\leqslant 31/2$ we find the relation $R\approx R_x$, which indicates the structure in the cranking regime. At low spins of the α_{f2} band we find $R>R_x$, while at higher spins the relation gradually changes into $R\approx R_x$. The nature of the bands close to the yrast line calculated for the present set of parameters seems to be much more complicated than that in the preceding subsection. Correspondingly, it is not easy to identify the candidates for the $n_w=2$ and 3 excitations in the case of $\gamma=-30°$, even when the most favorable degree of the high-j shell filling is chosen.

The coupling scheme of the quasiparticle and core angular momenta in the $(\alpha_f,\ n_w=0)$ and $(\alpha_u,\ n_w=1)$ bands, which

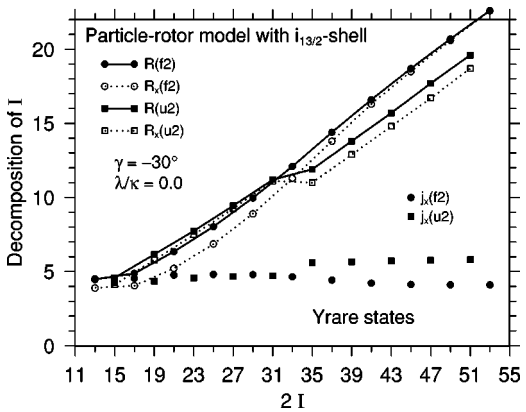

FIG. 8. Calculated values of R, R_x, and j_x, which are defined by Eq. (8), are plotted for the α_{f2} and α_{u2} bands.

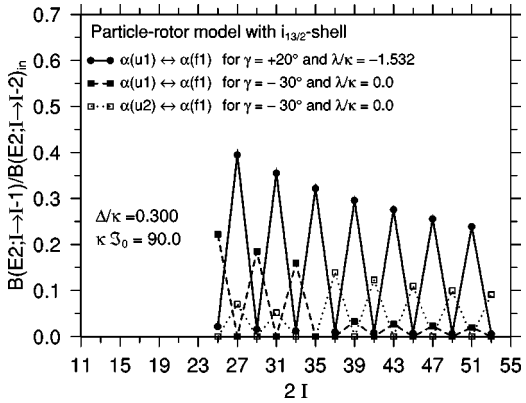

FIG. 9. Calculated $B(E2;I\rightarrow I-1)/B(E2;I\rightarrow I-2)_{in}$ values between the lowest-lying bands as a function of I. For $\gamma=-30°$ the α_{u1} and α_{u2} bands cross with each other between $I=31/2$ and 35/2. See the text for details.

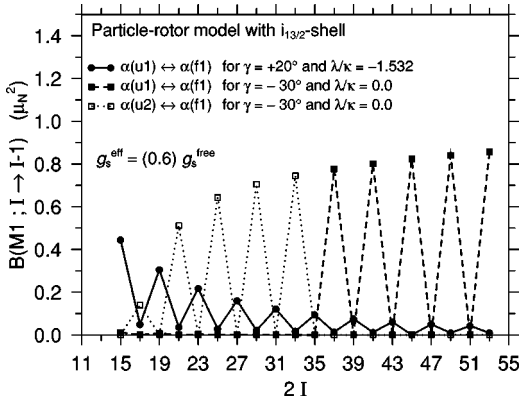

FIG. 10. $B(M1;I\rightarrow I-1)$ values calculated using $g_s^{eff}=0.6g_s^{free}$ are plotted for the transitions between the lowest-lying bands as a function of I.

is sketched in Fig. 4, is valid also for $\gamma=-30°$. However, the zigzag pattern of $B(E2;I\rightarrow I-1)$ values for the wobbling excitations as a function of I is out of phase compared with the case of the previous subsection. Namely, in the case of $\gamma=-30°$ the $B(E2;\alpha_f,n_w=0,I\rightarrow\alpha_u,n_w=1,I-1)$ values are large because the contributions from Q_0 and Q_2 coherently contribute to the $E2$ transitions, while $B(E2;\alpha_u,n_w=1,I+1\rightarrow\alpha_f,n_w=0,I)$ values are proportional to $(\hat{Q}_0)^2$, which vanishes for $\gamma=-30°$.

C. Comparison between the cases of ($\gamma=+20°$ and $\lambda/\kappa=-1.532$) and ($\gamma=-30°$ and $\lambda/\kappa=0.0$)

In Fig. 9 the calculated $B(E2;I\rightarrow I-1)/B(E2;I\rightarrow I-2)_{in}$ values between the lowest-lying bands are shown as a function of I. The larger $B(E2;I\rightarrow I-1)$ values in the zigzag pattern expressed by the filled (open) squares for $I<35$ ($I>35$), of which the larger values vary from 0.22 to 0.091, are for the $\Delta n_w=-1$ transitions for $\gamma=-30°$. Those values are about a factor of 2 smaller than filled circles, which are for the $\Delta n_w=-1$ transitions for $\gamma=+20°$, simply because the $B(E2;I\rightarrow I-2)_{in}$ values are about a factor of 2 larger for $\gamma=-30°$ than for $\gamma=+20°$. The $B(E2;I\rightarrow I-1)$ values for the $\Delta n_w=-1$ transitions are indeed about the same order of magnitudes for both γ values. It is seen that the smaller $B(E2;I\rightarrow I-1)$ values in the zigzag pattern are small for $\gamma=+20°$, while those for $\gamma=-30°$ are exactly zero due to the r_H quantum number. The $B(E2;I\rightarrow I-1)$ values in the zigzag pattern expressed by open (filled) squares for $I<35$ ($I>35$) are for the transitions in the cranking regime for $\gamma=-30°$, in which the zigzag pattern is out of phase compared with wobbling $\Delta n_w=-1$ transitions for the same value of $\gamma=-30°$. It is also noted that the zigzag pattern of the $B(E2;n_w=1,I\rightarrow n_w=0,I-1)$ values in the wobbling regime is out of phase between $\gamma=+20°$ and $\gamma=-30°$

When the α_{u1} band belongs to the cranking regime, the characteristic features in the $\Delta I=1$ electromagnetic transitions between the α_{u1} and α_{f1} bands, which are valid irrespective of γ values, are summarized as follows [2,6]: (a) the $B(E2;I\rightarrow I-1)$ values are the order of $1/I^2$ in the limit of large I values; (b) $B(M1;\alpha_{f1},I\rightarrow\alpha_{u1},I-1)$ values are relatively large being of the order of 1 μ_N^2, while $B(M1;\alpha_{u1},I+1\rightarrow\alpha_{f1}I)$ values are reduced.

In Fig. 10 the $B(M1;I\rightarrow I-1)$ values calculated using $g_s^{eff}=0.6g_s^{free}$ are plotted for the transitions between the lowest-lying bands as a function of I. The larger $B(M1;I\rightarrow I-1)$ values in the zigzag pattern expressed by open (filled) squares for $I<35$ ($I>35$), which reach 0.86 at $I=53/2$ are for the transitions in the cranking regime. It is seen that the smaller $B(M1;I\rightarrow I-1)$ values in the zigzag pattern are small for $\gamma=+20°$, while those for $\gamma=-30°$ are exactly zero due to the r_H quantum number. For $\gamma=-30°$ the $B(M1;I\rightarrow I-1)$ values between the yrast and wobbling excitation bands are very small in any case.

In Fig. 11 we schematically illustrate the $\Delta I=1$ $E2/M1$ transitions between lowest-lying bands for $\gamma=+20°$ and $-30°$, taking the most favorable degree of the high-j shell filling in respective cases. Since the intrinsic configuration of the maximally aligned particle is realized in the yrast spectra, the signature splitting in energy between the α_{f1} and α_{u1} band is qualitatively the same for the two γ values and is independent of whether the α_{u1} band belongs to the wobbling or cranking regimes. In the wobbling ($\Delta n_w=1$) transitions for $\gamma=+20°$ the signature dependence (or the zigzag pattern as a function of I) of the $B(E2)$ and $B(M1)$ values are in phase. Moreover, larger $B(E2)$ and $B(M1)$ values occur for the transitions with larger transition energies, in which the $E2$ transitions are dominant. In contrast, in the wobbling ($\Delta n_w=1$) transitions for $\gamma=-30°$ the zigzag pattern of the $B(E2)$ and $B(M1)$ values is out of phase. For the transitions with larger transition energies the $B(E2)$ values vanish and the $B(M1)$ values are very small, while for the transitions with smaller transition energies the $B(E2)$ values are large and the $B(M1)$ values vanish. On the other hand, if the α_{u1} band belongs to the cranking regime in the case of $\gamma=-30°$, for the transitions with larger transition energies the $B(E2)$ values are small and the $B(M1)$ values vanish, while for the transitions with smaller transition energies the $B(E2)$ values vanish and the $B(M1)$ values are large.

In order to understand the dependence of the possible appearance of wobbling excitations on γ values, in Fig. 12 we

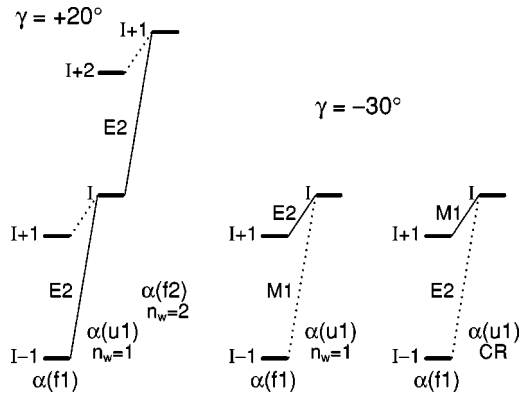

FIG. 11. Schematic illustration of the $\Delta I=1$ $E2/M1$ transitions between the lowest-lying bands for $\gamma=+20°$ (the wobbling regime with the yrast, $n_w=1$ and $n_w=2$ bands) and for $\gamma=-30°$ (at the left the wobbling regime for the α_{u1} band, while at the right the cranking regime), taking the most favorable degree of the high-j-shell filling in respective cases. Stronger transitions are expressed by solid lines, while weaker transitions are denoted by dotted lines. The type of the dominant transition, $E2$ or $M1$, is indicated for respective transitions. In the case of $\gamma=-30°$ the other type ($E2$ or $M1$) of the transition, which is not written, exactly vanishes due to the presence of the r_H quantum number. The signature splitting in energy may happen to be such that the (α_{u1},I) state lies below the $(\alpha_{f1},I+1)$ state, however, the energy difference between the (α_{u1},I) and $(\alpha_{f1},I+1)$ states is always smaller than the one between the (α_{u1},I) and $(\alpha_{f1},I-1)$ states.

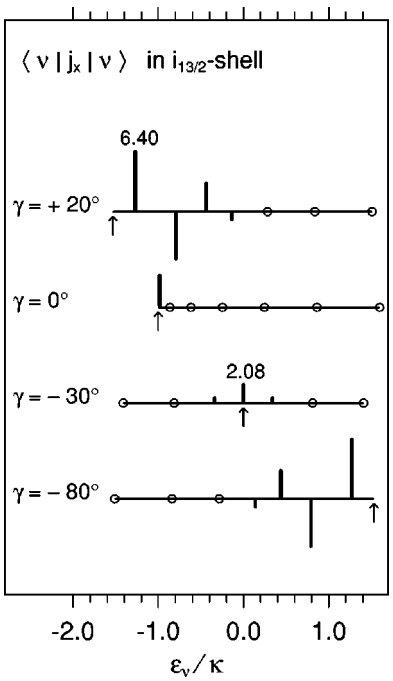

FIG. 12. One-particle energy eigenvalues and the positive or negative expectation values of j_x in the $i_{13/2}$ shell for the favored signature and various γ values, before rotation sets in. Instead of writing the scale of the vertical axis, the value of $\langle j_x\rangle$ is indicated in two places as 6.40 and 2.08. The eigenvalues of the states, which have either vanishing or negligible $\langle j_x\rangle$ values, are denoted by open circles. The position of the λ value, which is given by Eq. (4) for the respective γ values, is indicated by thin arrows.

plot the one-particle energy eigenvalues and the expectation values of j_x in the high-j ($=i_{13/2}$) shell for the favored signature and various γ values before rotation sets in. Instead of writing the scale of the y axis, numerical values of $\langle j_x\rangle$ are indicated in two places. The eigenstates, which have either vanishing or negligible $\langle j_x\rangle$ values, are denoted by open circles. By thin arrows the position of λ value, which is given by Eq. (4) for respective γ values, is indicated. As rotation sets in, it is easy for the lowest-lying quasiparticle to get a full alignment for $\gamma=+20°$ and $-80°$ with respective Fermi levels indicated by arrows, if Δ/κ is the order of 0.3. In contrast, a faster rotation is needed in the case of $\gamma=-30°$. Since at high spins the rotational energy dominates over the intrinsic energy, the wobbling regime will become energetically more expensive than the cranking regime at a certain spin. Thus, for $\gamma=-30°$ it is more difficult to obtain wobbling mode in a clean form near the yrast line, even if the triaxial shape is equally supported by the core.

IV. CONCLUSIONS AND DISCUSSIONS

Using the particle-rotor model in which one quasiparticle in the high-j ($=i_{13/2}$) shell is coupled to the core of triaxial shape, possible wobbling phonon excitations, which may appear close to the yrast line, are studied. Choosing the most favorable degree of high-j shell filling, in which aligned particles appear in the yrast line at spins as low as possible, the structure of the yrast bands with triaxial shape is analyzed.

The wobbling phonon excitations are characterized by the intrinsic structure very similar to that of the basis band, on which the wobbling excitations are built, while the angular momenta of collective rotation show the wobbling features. Thus, the wobbling bands built on the yrast band may be experimentally identified by: (a) very similar moments of inertia and spin alignments; (b) strong $B(E2;I\rightarrow I-1)$ values for $\Delta n_w=1$ transitions, which may dominate over $M1$ components. The signature dependence of the $B(E2;I\rightarrow I-1)$ values as a function of I (or the zigzag pattern) depends on the region of γ values, $-120°<\gamma<-60°$ or $-60°<\gamma<0°$ or $0°<\gamma<+60°$.

We have found that the wobbling phonon excitations along the yrast line can be more easily observed for the Fermi level lying below the high-j shell with most favorable triaxiality $\gamma\approx+20°$ than that lying around the middle of the shell with $\gamma\approx-30°$.

The wobbling motion described in the present paper is strongly related to the shell structure of the nucleus and can appear at relatively low angular momenta. The nuclear shell structure favors a particular (triaxial) shape depending on angular momenta as well as the neutron and proton numbers. In order to realize the wobbling mode studied in the present work, it is absolutely necessary that the core particles strongly favor approximately the same triaxial shape as that favored by aligned particles. In such a case the total system can keep almost the same triaxial shape in the wider region of angular momentum, and the wobbling phonon excitation bands may be easily realized.

Comparing our numerical result presented in Sec. III A with the fact that in ^{163}Lu the crankinglike α_{u2} band has not been experimentally observed in the neighborhood of the yrast line, it is likely that our present simple model does not give a very quantitative estimate of the intrinsic-energy difference between the crankinglike and wobblinglike regimes. The dependence of both the pair correlation and moments of inertia on I must be also included in the model calculation, in order to make a further quantitative comparison with experimental data.

ACKNOWLEDGMENTS

The author expresses her sincere thanks to Gudrun Hagemann for informative communications. She is grateful to Crafoordska stiftelsen for financial support, which made it possible to carry out the present research work.

[1] A. Bohr and B. R. Mottelson, *Nuclear Structure* (Benjamin, Reading, MA, 1975), Vol. II.
[2] S. W. Ødegård *et al.*, Phys. Rev. Lett. **86**, 5866 (2001).
[3] E. R. Marshalek, Nucl. Phys. **A331**, 429 (1979).
[4] I. Hamamoto and B. R. Mottelson, Phys. Lett. **127B**, 281 (1983).
[5] I. Hamamoto, Phys. Lett. B **193**, 399 (1987).
[6] D. R. Jensen *et al.*, Nucl. Phys. (to be published).
[7] G. B. Hagemann (private communication).
[8] C. G. Anderson *et al.*, Nucl. Phys. **A268**, 205 (1976).
[9] I. Hamamoto, Nucl. Phys. **A520**, 297c (1990).
[10] A. Schmidt *et al.*, Eur. Phys. J. A **2**, 21 (1998), and references quoted therein.
[11] Y. R. Shimizu and M. Matsuzaki, Nucl. Phys. **A588**, 559 (1995).
[12] I. Hamamoto, Nucl. Phys. **A271**, 15 (1976).
[13] I. Hamamoto and B. R. Mottelson, Phys. Lett. **132B**, 7 (1983).
[14] M. Matsuzaki, Y. R. Shimizu, and K. Matsuyanagi, Prog. Theor. Phys. **77**, 836 (1988).